AIAA 80-1433R

Flow and Discharge Characteristics of Electron-Beam-Controlled Pulsed Lasers

B. N. Srivastava,* G. Theophanis,† and R. Limpaecher†
Avco Everett Research Laboratory, Inc., Everett, Mass.
and
J. C. Comly‡
Los Alamos Scientific Laboratory, Los Alamos, N. Mex.

Discharge and flow characteristics of an electron-beam-controlled pulsed CO_2 laser are investigated. Several specific discharge issues for the device, such as ionization source uniformity, electric field uniformity, energy deposition uniformity, and discharge confinement are addressed by developing a self-consistent numerical solution of the laser discharge problem. These solutions include the effects of finite electron beam, finite electrode length, and arbitrary electrode shape. The effect of coupling between the cavity acoustics and the discharge is modeled using a general transient two-dimensional nonlinear approach. Results are presented to demonstrate the effect of this coupling during a pulse time.

I. Introduction

THE recent drive to high average power and high energy per pulse lasers has been enhanced by the invention of many scalable laser excitation methods. This paper deals with a general class of electric excitation lasers commonly known as "electron-beam-controlled" lasers. This technique for discharge control in CO_2 lasers was first demonstrated by the pulse-sustainer laser[1] which lead to the electron-beam sustainer lasers.[2,3] Further scaling of such devices could lead to many other interesting applications, such as laser fusion,[4] and therefore there is a need to develop an understanding of such discharges. This paper is an attempt toward achieving this goal.

In an electron-beam-controlled discharge laser the electron beam passes through a foil, a grid structured electrode (cathode, to provide transparency to the electron beam), and a working gas medium (see Fig. 1). Due to the electron beam scattering, energy loss and the electric field effect a volume ionization which may be larger in physical extent than desired (i.e., ionized gas outside the desired working volume) may be produced resulting in significant reduction of the electrical efficiency for the device. These effects may also produce a plasma within the working region that is to some degree nonuniform. A direct result of these nonuniformities is its adverse effect on the optical quality of the output laser pulse. An analysis of this problem is, therefore, necessary in order to achieve significant improvement in the overall efficiency and performance of such devices.

There have been several theoretical efforts in the past to address these issues.[5-9] However, most of these attempts are approximate. A fairly good description of the approximations involved in various previous attempts is given in Ref. 10. The general attempt[10,11] has been to determine the ionization-source distribution using Monte-Carlo simulation of the laser cavity and then determine the electric-field distribution using "stream tube" approximation of Ref. 5. However, this approach is based on a linear perturbation analysis of the current conservation equation. For this reason this approach may provide erroneous results for cases where the perturbation parameter ($\epsilon \sim$ ratio of the electric field parallel and perpendicular to the main flow direction) is large. This may happen due to nonuniformities in the ionization source, electrode roll-off, and other effects. A more accurate theoretical approach would be that reported in Ref. 9 where the current conservation equation was solved numerically to determine the discharge-field distribution. This approach, however, utilized an approximate ionization-source distribution that was determined using a diffusion theory.[12] This theory is based on the assumption that on the average an electron loses as much energy during an average collision as it gains from the applied electric field. This technique would work well provided the implicit assumption is valid. However, our recent calculations for large input energy lasers indicate that the energy gained by the primary electrons due to the applied field is much larger than the energy lost due to the collision processes. A natural extension of this method is, therefore, required for such electron-beam-controlled pulsed lasers. The subject matter of this paper deals with such an extended theoretical approach.

The discussion outlined in the preceding paragraphs assume an isodensity gas mixture in the laser cavity. Nonuniformities in the gas density affect the discharge and deposition uniformities. This coupling between the cavity fluid and plasmadynamics occurs through the dependence of the plasma conductivity on the laser gas density.[13] Density nonuniformities in the laser cavity may be caused by the boundary layers (if any) near the side walls, the jet mixing zone near flow plate, heating effect of the laser gas, and the acoustic waves caused by the edge effects (discontinuous energy deposition). The first two effects are confined (by design) outside the active volume of the laser cavity and the third effect is generally small during a pulse time. The last of these effects is important and could result in a thermal instability of the discharge. A previous attempt to address this instability utilized a linear approach[14] in one dimension. We have analyzed this problem using a two-dimensional transient numerical technique in order to evaluate the gas density decay rate (leading to thermal instability) due to coupling between plasma and fluid dynamics.

The present paper is divided into several parts. Section II deals with the analysis of the discharge and the modeling description. Section III deals with the results on source uniformity studies, discharge uniformity, and discharge confinement. The next section, Sec. IV, details the coupling effect of fluid and plasma dynamics in the laser cavity.

Presented as Paper 80-1433 at the AIAA 13th Fluid and Plasma Dynamics Conference, Snowmass, Colo., July 14-16, 1980; submitted July 22, 1980; revision received Jan. 30, 1981.

*Principal Research Scientist. Member AIAA.
†Principal Research Scientist.
‡Scientist.

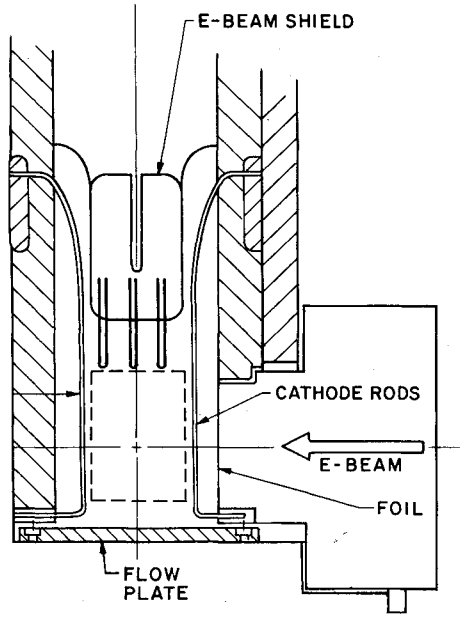

Fig. 1 Components of a laser discharge cavity.

Relevant modeling, numerical approach, and the results of this analysis are outlined in this section.

II. Analysis of the Discharge

The generic components of a typical laser discharge cavity are shown in Fig. 1. The cavity discharge region is confined by using a bladed e-beam shield as depicted in Fig. 1. The dotted line in this figure shows the active volume of the laser cavity. It is in this volume where ionization and discharge uniformity is desired.

The cavity discharge is modeled as a nonuniform, nonlinear, two-dimensional resistor between the anode and the cathode. Mathematically this is described as

$$\nabla \cdot \sigma(\nabla \phi) = 0 \tag{1}$$

where

$$E = -\nabla \phi \tag{2}$$

where ϕ is the potential, σ the conductivity, and E the electric field. Equation (1) is nonlinear because σ is a function of the electric field. For the present discharge problem σ is unknown a priori. This can be determined by the following expression:

$$\sigma = c(E/N)^{0.328}\sqrt{S} \tag{3}$$

where N is the neutral gas number density and S the ionization rate caused by the high energy electron beam. Equation (3) has been determined for a recombination dominated discharge with 3/1/0.08 N_2, CO_2, H_2 mixture at 220 K.[15] The nature of the source function S has been studied previously in detail.[16,17] The physics of electron scattering and transport have been described in these references using Bethe's age diffusion theory[18] for diffuse electrons. The age diffusion theory has also been modified previously to include the effects of electric and magnetic fields.[19] However, these theories are based on the assumption that the high energy electrons in traversing through the gas medium lose, on the average, as much energy as they gain from the electric field. Previous calculations requiring coupling of ionization source function and the discharge problem have been achieved by using this age diffusion source formula.[9] The results so obtained have been found to compare well with the experimental data for small scale discharges.[9] However, it has been determined that the age diffusion theory is only approximate for discharges where the electrons on the average gain a much larger amount of energy than they lose between successive collisions. This

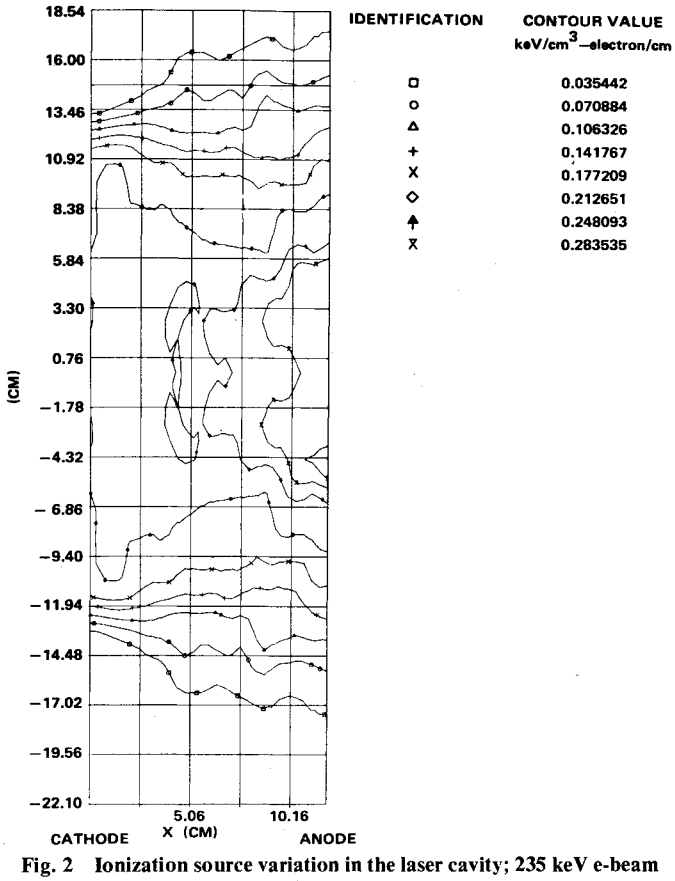

Fig. 2 Ionization source variation in the laser cavity; 235 keV e-beam energy with anode backscattering.

results in the breakdown of the diffusion theory. It was, therefore, found necessary to obtain the ionization source function more accurately by using numerical solutions of the transport equations. This can be most suitably obtained by using Monte-Carlo techniques. We have used a modified version of the Monte-Carlo computer code for the source function which was developed at Los Alamos Scientific Laboratory.[20] Details of the physics, relevant equations, and the numerical techniques used in the code are described in Refs. 20 and 21.

In order to obtain a self-consistent solution of the energy deposition problem under consideration, a coupled solution of Eqs. (1) and (3) with the ionization source S, determined from the Monte-Carlo code, is required. This was done for our analysis where the effects of the electric and magnetic fields on the high energy electrons are determined in an iterative sense. This procedure involves using the Monte-Carlo code with an average (constant) electric field and average (constant) discharge current (and associated magnetic field). The resulting ionization source distribution is used to determine the electric-field distribution by solving Eq. (1) for a given geometry and boundary conditions.[22] Equation (1) is solved by using a finite-element method[23] that utilizes four-node quadrilateral elements for most of the mesh. Triangular elements, however, are occasionally used on boundaries to avoid severe mesh distortions. The basic program incorporating this technique was developed by Sackett.[24]

III. Results and Discussion of Discharge Calculations

Due to the complexity of this general problem and also to understand the impact of various parameters on the laser design, it will be our approach to analyze various aspects of the problem in series. We will first analyze the ionization source uniformity due to the primary e-beam under various conditions and then discuss the corresponding discharge

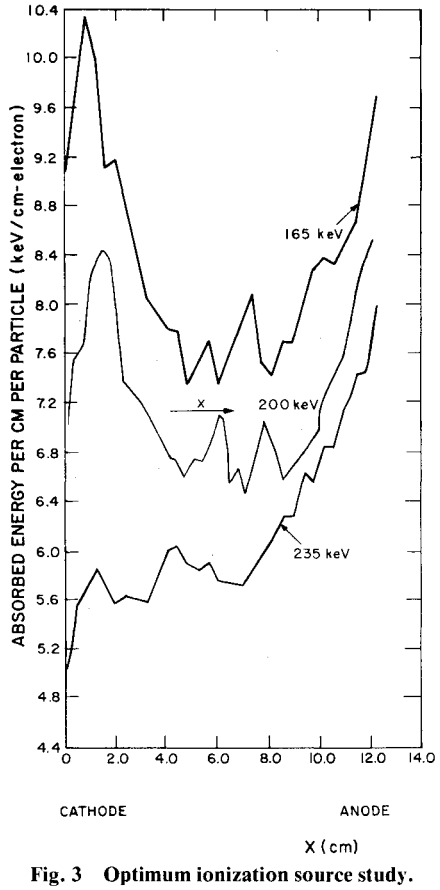

Fig. 3 Optimum ionization source study.

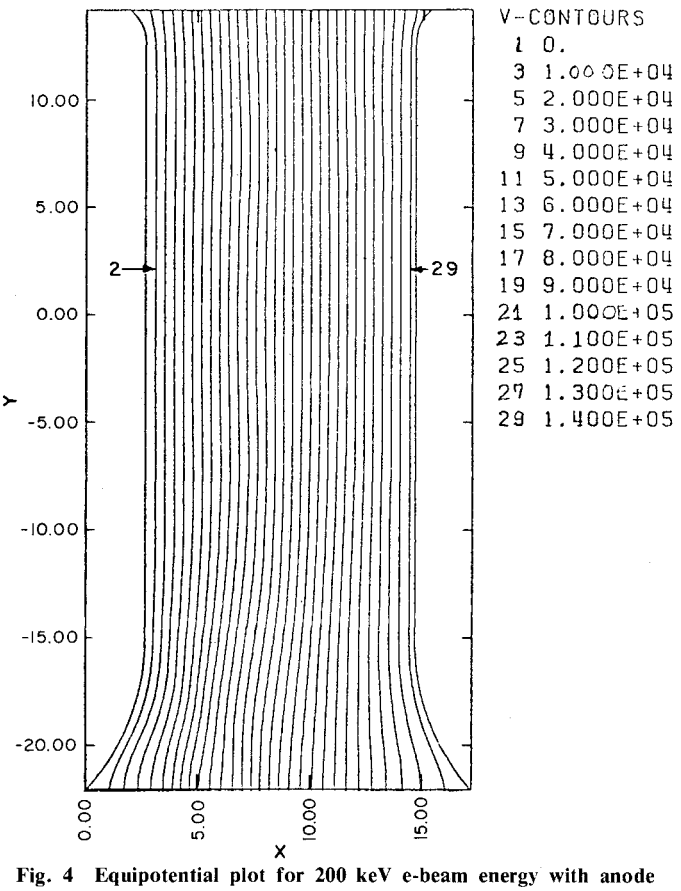

Fig. 4 Equipotential plot for 200 keV e-beam energy with anode backscattering.

uniformity for these conditions. The motivation for these studies is to identify conditions that would result in an optimum performance for the device. We will also address some issues associated with discharge confinement, in particular, the stress on the blades that are used to confine the discharge (see Fig. 1). An assessment of its effect on the active volume discharge characteristics will be made.

Ionization-Source Uniformity

Using the approach outlined in the preceding section, we have studied the ionization-source function for the laser discharge problem shown in Fig. 1 without the bladed e-beam shield. The effect of the bladed e-beam shield will be discussed later. We have modeled the foil (1 mil-Al), the applied voltage between anode and cathode (12 cm apart, 148 kV), foil-cathode separation (1.6 cm), laser gas mixture (3/1/0.08, N_2, CO_2, H_2 at 220 K, 1 atm), and backscattering from anode (aluminum). Figure 2 shows a contour plot of the ionization-source variation in the cavity for an electron beam voltage of 235 keV and a solid anode. It is observed from this figure that the ionization-source distribution in the cavity is influenced significantly due to the backscattering of the primary electrons from the solid anode. The backscattered electrons influence more than half the discharge dimension from the cathode to anode. Further analysis of our results show that the primary electrons gain a significant amount of energy as they travel through the gas medium due to the large sustainer voltage. This results in backscattered electrons from the anode which are highly energetic. Since these backscattered electrons travel against the electric field, they deaccelerate rapidly losing all their energy to the gas. It has been pointed out before[7] that backscattering from the anode can be used advantageously to achieve source uniformity, however, the results of our calculations show that the adverse effect could also result at high sustainer and electron-beam voltages. An optimization between anode material, its transparency, and the operating conditions is, therefore, required to ascertain proper ionization-source uniformity. We have performed a limited study to optimize the ionization-source function relative to the electron-beam voltage, keeping all other parameters fixed for a solid anode situation (for our device this was considered to be the appropriate model). The result of this study is shown in Fig. 3 where the integrated one-dimensional ionization profile (integrated in y direction) is shown as a function of the distance from the foil to anode. Three different cases with electron-beam voltages of 165, 200, and 235 keV is shown. It is observed that the optimum source uniformity is obtained by operating at about 200 keV for these conditions.

Discharge Field and Energy Deposition Uniformity

Uniformity of the ionization source in a laser cavity contributes toward the uniformity of the energy deposition. Using our discharge computer code we have analyzed the details of the electric-field distribution in the laser cavity in an effort to identify and eliminate any undesirable regions of stress concentration within the laser cavity. Figure 4 shows the equipotential lines for the cavity that is shown in Fig. 1 (without the bladed e-beam shield). The electron-beam voltage for this case was the optimized voltage of 200 keV. It is observed from this figure that the equipotential lines tend to be pulled toward the cathode and compress together at downstream points in the cavity. Further analysis of the computational results shows that this effect is caused by the fact that this zone lies in the shadow region of the electron-beam path. The gas in this region is relatively un-ionized and therefore the electric field is higher. This results in equipotential lines being pulled toward the cathode. Our calculations further show that the severity of this stress concentration increases with increasing electron-beam voltage. This is because at lower electron-beam voltage the electron scattering is higher which results in a more uniform ionization in the shadow region than it would be for a higher e-beam voltage. At the upstream side this situation does not

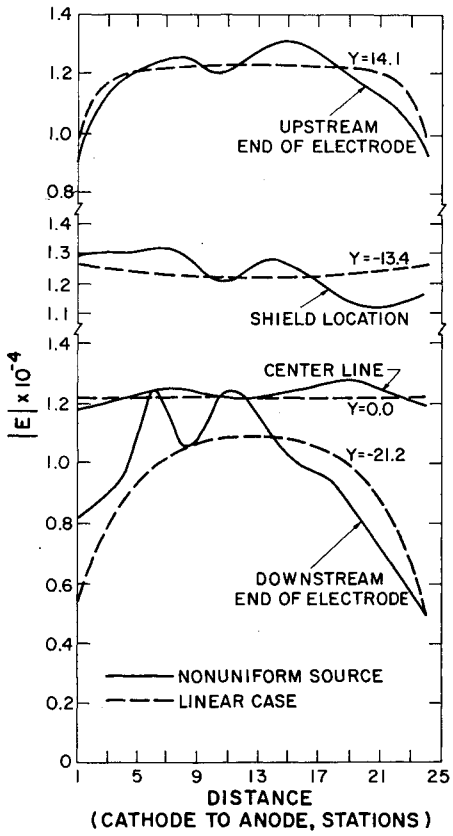

Fig. 5 Electric field distribution in the laser cavity, with anode backscattering.

arise because the shadow region of the electron-beam path is terminated by the flow plate that confines the discharge. In some discharges this stress enhancement may become critical to avoid initiation of arcing in the cavity. For our study this region was not of interest because we intended to shield this region by the use of electron-beam shield as shown in Fig. 1. This shielding effect will be discussed later in this section. A reasonable conclusion based on this study is that there is a potentially critical stress concentration region downstream of the cavity (without e-beam shield). The magnitude of this stress enhancement can be controlled to some degree by proper choice of the operating point. Our study has been limited to a fixed sustainer voltage, electrode shape, and other discharge parameters. However, based on the analysis of our results, it is anticipated that this stress enhancement effect would be present for most laser discharges to some extent if the electrodes extend in the regions of relatively un-ionized gas caused by the shadow effect of the electron-beam scattering.

It will be instructive to show the field variation in the laser cavity at different locations for the optimized case. This is shown in Fig. 5 where the magnitude of the field ($|E|$) is shown at different y locations as one moves from the cathode to anode. In order to assess the extent of the effect of ionization-source nonuniformity on the field distribution, we have also shown the ideal discharge case where the ionization-source term is uniform and the gas conductivity is independent of the electric field (linear case, considered to be ideal). Notice that at the centerline of the cavity, there is no appreciable variation of the electric field for our optimized nonuniform source. This result is a direct consequence of our effort to optimize the source uniformity. At the upstream end (near flow plate) at $t = 4.0$ cm the variation of the electric field from cathode to anode is primarily due to the electrode shape. The effect of source nonuniformity increases as one moves further downstream. At $y = -13.4$ cm, which is the proposed location of our e-beam shield, the field variation from cathode to anode is restricted to less than 10%. At the downstream end of the electrode ($\sim y = -21.2$) the field variation is again primarily due to the shape of the electrode (increased discharge gap). Our calculations for the energy deposition using the optimized e-beam voltage shows that the discharge heating uniformity is fairly good for most parts of the active volume of the cavity except for the edge effects. Our similar calculations with an unoptimized case show a more nonuniform distribution than that for the optimized case.

Discharge Confinement

In the interest of electrical efficiency, the laser discharge must be confined to the active laser volume. We have achieved this in the past[25] by using an n-bladed insulator shield. In our current device, we utilize the same concept, as shown in Fig. 1. An understanding of the effect of this type of bladed shield on the laser discharge is important in order to improve the overall performance of the laser cavity. In general the stress enhancement on these blades may limit the energy loading ability of the laser cavity. A limited effort has been made to model these shields and to study their impact on the laser cavity stress distribution. An understanding of the stresses caused by these shields may lead to a properly designed shield in order to prevent/delay arcing in the laser cavity. There are several issues that could complicate the prediction of stress enhancement on these shields. A complete analytical solution of all the processes involved would be quite complex. This would especially be true if an attempt is made to include the effects of surface charges. Near the insulator boundaries there may be a sheath of small thickness where physical processes are more complex (possibly similar to what is observed near plasma probes[26]). In the simple analysis shown here these effects have been neglected.

One of the problems that we faced in modeling the e-beam shield was the evaluation of the "shadow effect" (caused by the electron beam not penetrating the spacing between two successive blades). Our difficulty was mainly due to the inability of our present code (ionization source code) to account for the protruding solid blades in the path of the primary e-beam electrons. Our first attempt was, therefore, directed toward understanding the effect of this shadow region on the overall stress distribution. For this purpose a simple model problem with all the characteristics of our actual laser discharge problem was formulated.

Figure 6a shows the details of the model problem. The normalized source distribution shown in this figure was assumed to drop linearly on the electron-beam side of the insulator surface while an exponential decrease in ionization source was arbitrarily chosen to model the shadow effect. Two different exponents of the exponential drop were chosen to establish the sensitivity of this shadow region on the stress distribution at the surface of the insulator blade. The results of this model problem study are shown in Fig. 6b where the stress distribution on the surface of the insulator blade is plotted. The cases that are shown in this figure are that of a linear case ($m = 0$, $s = \text{const}$; see Fig. 6b), uniform source nonlinear case ($m = 0.328$, $s = \text{const}$), and the two cases of shadow effect ($s \sim e^{-x}$ and $s \sim e^{-5x}$). It is observed from this figure that the stress distribution on the surface of the insulator shield can be well approximated (within about 10-14% of peak stress) by a linear solution. Physically these results merely signify that when an insulator e-beam shield is introduced in a discharge region the stress is governed more by perturbations caused by the insulators shape, thickness, etc. than nonlinearity of discharge and nonuniformity in the source. An analysis of the complete laser discharge problem with a 3-bladed shield was considered relevant to support the findings of the simple model problem. Figure 7a shows the equipotential plot for our laser discharge problem of Fig. 1. We have used the ionization-source distribution obtained from our Monte-Carlo code everywhere except in the shadow regions where there is an exponential drop taken from the tip

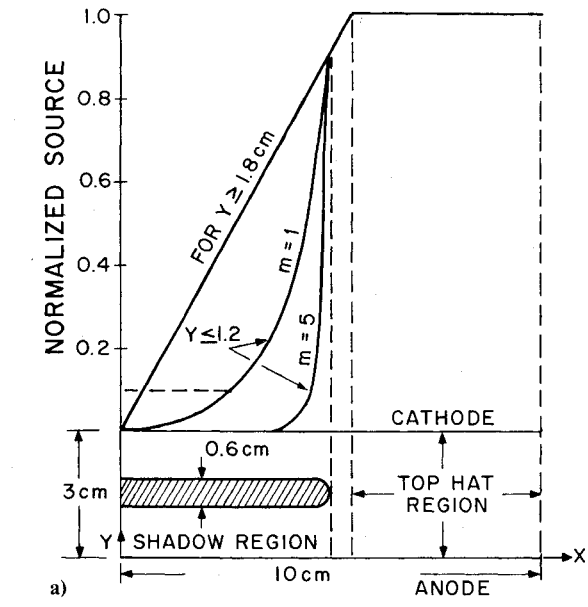

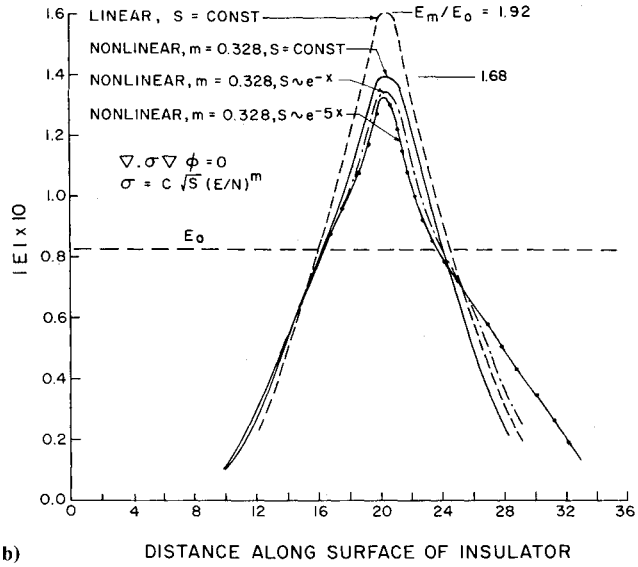

Fig. 6 a) Model problem study for an insulator e-beam shield, b) stress distribution on the insulator blade for the model problem.

of the insulator blade to the tail end of the blade. Figure 7b shows the stress variation from cathode to anode near the tip of the insulator blade. Once again results are similar to the model problem. The results from this analysis have an interesting impact on the design of insulator blades in order to confine discharges. First it is apparent that a design based on linear analysis will be sufficient. The cost of computations for design optimizations would be far less expensive compared to the nonlinear, nonuniform case. It is also quite evident that the insulator blades tend to shield effectively the discharge zone toward the tail end. This in effect implies that the insulator mountings and the triple point (where the electrode terminates creating a triple-point junction between electrode, dielectric mounting, and laser ionized gas) would lie in zones of very small stresses. It would not be necessary, therefore, to carefully design them since stresses at these points would be of no concern. The peak stress occurs at the nose of the insulator blades and this stress concentration may be the critical issue to initiate arcing in the laser cavity. Under such circumstances, a designer would be interested in redistributing these stresses through a more careful design and analysis. This aspect of the problem is beyond the scope of the present paper.

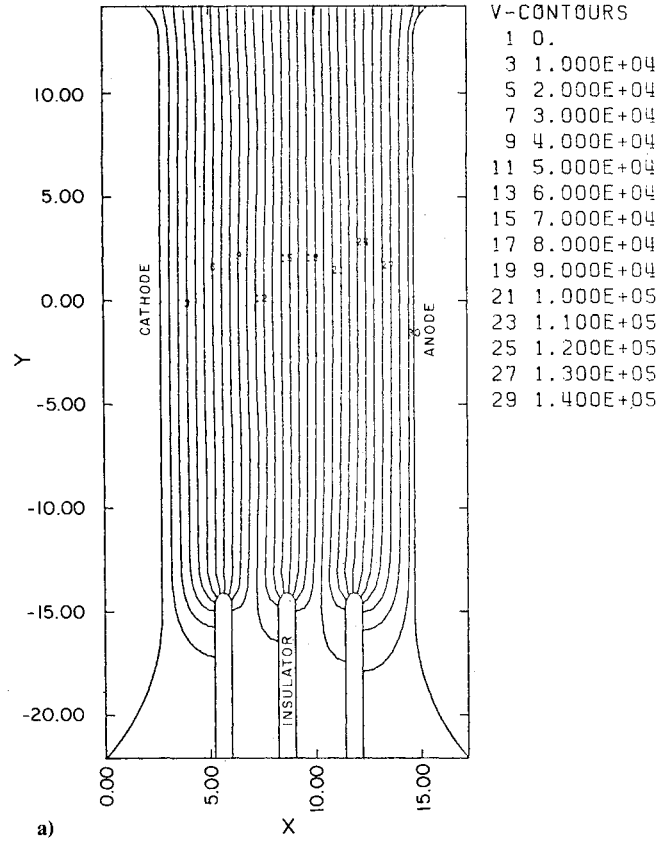

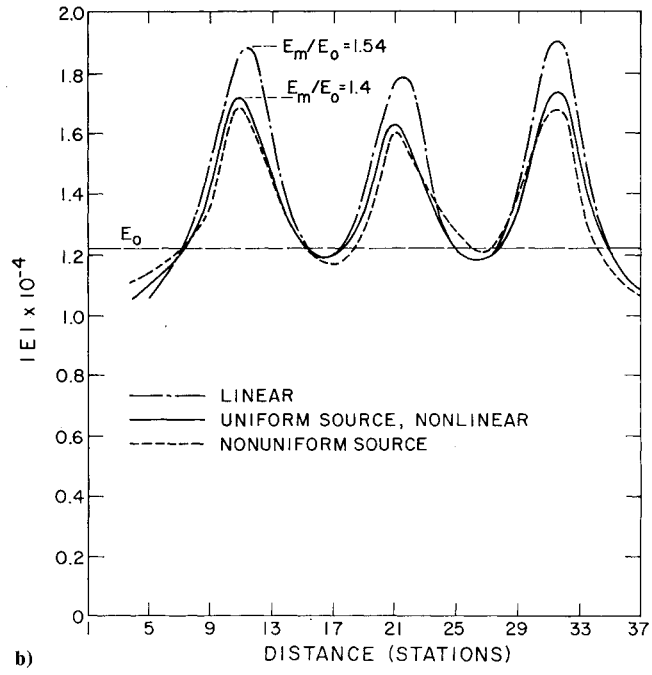

Fig. 7 a) Equipotential lines in the laser cavity with 3-bladed e-beam shield (200 keV e-beam energy with anode backscattering); b) stress from cathode to anode near 3-bladed shield.

IV. Plasma and Fluid Dynamics

The discharge calculations and discussions outlined earlier assume an isodensity gas mixture. In practice, however, the laser cavity fluid mechanics are quite complex and in some instances fairly nonuniform. This is specifically true near boundaries where acoustic waves are present during a pulse time.[27] Away from boundaries, the energy deposition process (gas heating) may also cause density perturbations; however, its effect on the discharge characteristics is generally small.

Near boundaries the coupling of the cavity fluid mechanics and plasma dynamics that takes place through the dependence of the local plasma conductivity on the local gas density may result in a thermal instability of the discharge. The objective of this section is to analyze this coupling process in order to quantify its effect. During a pulse time, when the discharge characteristics are of interest, severe acoustic disturbances could be generated in the laser cavity. These acoustic disturbances are caused by nonuniform heating of the laser gas primarily due to the other design requirements. For example, pulsed flowing gas lasers typically have laser cavities that do not extend all the way to the side walls bounding the flow region, as shown in Fig. 1. This arrangement results in an almost discontinuous change in the sustainer energy deposition, causing an expansion wave to propagate from the cathode into the cavity. This situation may also be present behind the anode. This arrangement is further complicated by the fact that many high power pulsed CO_2 laser systems utilize an n-bladed e-beam shield (see Fig. 1) to confine the discharge and thereby improve its electrical efficiency. The effect of this shielding is to generate an expansion wave in the longitudinal direction, that moves toward the center of the cavity. During a pulse time, therefore, there will be a region of severe density drop that is identified by the presence of both longitudinal and transverse waves of the same nature (i.e., expansion). It will be expected, therefore, that the coupling between discharge and fluid mechanics will be enhanced greatly. This situation may also be present toward the flow plate side if there is a finite distance that separates the energy deposition zone and the flow plate. Under certain circumstances this severe density drop region may lead to a thermal instability of the discharge.[14] This problem has been analyzed previously using a linearized technique[14] for one-dimensional situations. Two-dimensional nonlinear effects will be of importance at high energy loadings of the laser discharge cavity, where strong compression and expansion waves are present. As stated earlier, the purpose of this section is to assess the impact of this coupling between plasma and fluid dynamics on the density decay rate. In an effort to keep the results of the analysis general, a parametric study is reported.

Theoretical Model

A two-dimensional nonlinear model is developed to study the density exponentiation process. This model is essentially a two-dimensional fluid-mechanical model with heat transfer. The conservation equations are written as

$$\frac{\partial \rho}{\partial t} + \frac{\partial}{\partial x}(\rho u) + \frac{\partial}{\partial y}(\rho v) = 0 \tag{4a}$$

$$\frac{\partial}{\partial t}(\rho u) + \frac{\partial}{\partial x}(p + \rho u^2) + \frac{\partial}{\partial y}(\rho u v) = 0 \tag{4b}$$

$$\frac{\partial}{\partial t}(\rho v) + \frac{\partial}{\partial x}(\rho u v) + \frac{\partial}{\partial y}(p + \rho v^2) = 0 \tag{4c}$$

$$\frac{\partial E}{\partial t} + \frac{\partial}{\partial x}[(E+p)u] + \frac{\partial}{\partial y}[(E+p)v] = \left[\frac{Q_r L}{\gamma p_r u_r}\right]\rho^{-n} \tag{4d}$$

$$p = (\gamma - 1)[E - \tfrac{1}{2}\rho(u^2 + v^2)] \tag{4e}$$

The preceding equations are written in a nondimensional form. The reference quantities are represented by p_r for pressure, u_r for velocity, Q_r for a characteristic heating term, and L is a characteristic length. The density exponent n is positive and γ is the ratio of specific heat for the laser mixture (assumed constant). It is observed from these equations that the nondimensional heating term

$$\bar{Q} = \left[\frac{Q_r L}{\gamma p_r u_r}\right]$$

as it appears in Eq. (4d) will be of importance. The two-dimensional transient density exponentiation process will be governed by this heating term and the exponent n.

We have analyzed the set of Eqs. (4a-e) for determining the density exponentiation process for various parametric values of $\bar{Q}$ and n. Numerical solutions were generated for the set of Eqs. (4a-e) using a flux corrected SHASTA shock capturing scheme.[28] Calculations were performed only within a pulse time since the deposition process is complete during this time. The effect of the jet mixing zone next to the flow plate was neglected to isolate the acoustic wave effects. Since the time of interest was short, the side boundaries and flow plate were assumed to be at large distances from the energy deposition zone. The bladed e-beam shield was not modeled from a fluid mechanical standpoint, however, its effect was considered by assuming that the discharge is confined effectively to the active volume. This resulted in assuming a top hat profile of the energy deposition ($\bar{Q}$) in both x and y directions. The transient behavior of the input energy was obtained from the V-I characteristics of our discharge. This gave us the approximate rise and fall time for the heating term.

The numerical solution outlined provides information on the one-dimensional and also on the two-dimensional aspects of the problem. The central part of the laser cavity is essentially one dimensional due to the short time involved. Only regions near the corners of the laser cavity are truly two dimensional. In order to understand the one-dimensional and two-dimensional aspects of the density exponentiation process, we have analyzed the computational results both at the centerline and toward the edges. It was considered essential to separate the two effects in order to assess the physical behavior of the exponentiation process. Figure 8 shows the density distribution (normalized to initial cavity density) in the cavity in the longitudinal direction for various values of the transverse distance at the end of a pulse time (20 μs). For this particular calculation the density exponent was taken to be $n = 0$, which indicates no coupling between plasma and fluid dynamics. It is observed from this figure that the wave system at this time consists of an expansion wave, followed by a spread out contact surface, and then a compression wave moving out of the cavity. This figure is of interest in order to determine the point of minimum density,

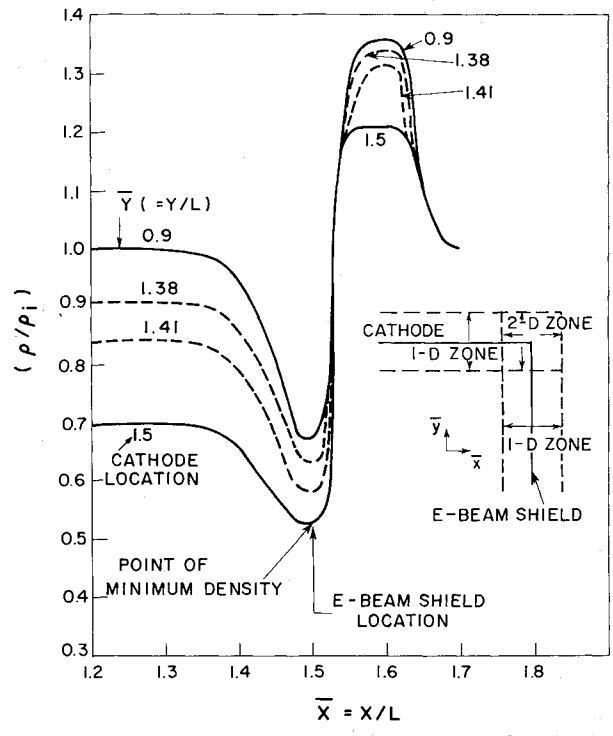

Fig. 8 Density variation in the laser cavity at the end of a pulse time.

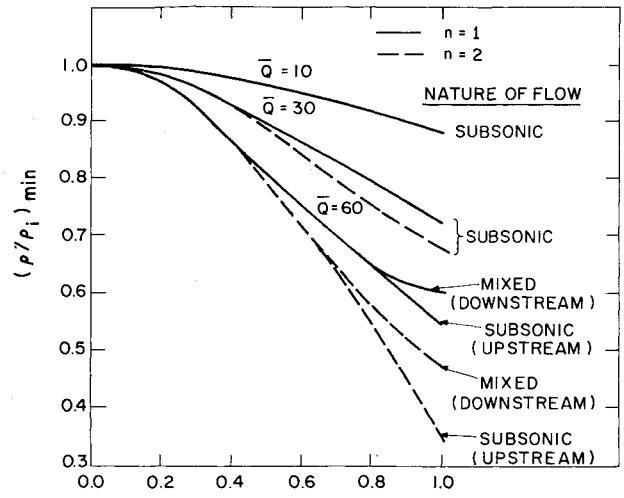

Fig. 9 One-dimensional effect of coupling between plasma and fluid dynamics in the laser cavity.

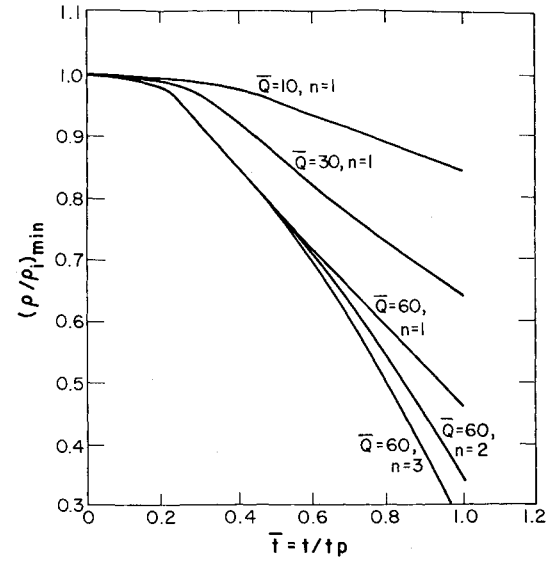

Fig. 11 Two-dimensional effect of coupling between plasma and fluid dynamics in the laser cavity.

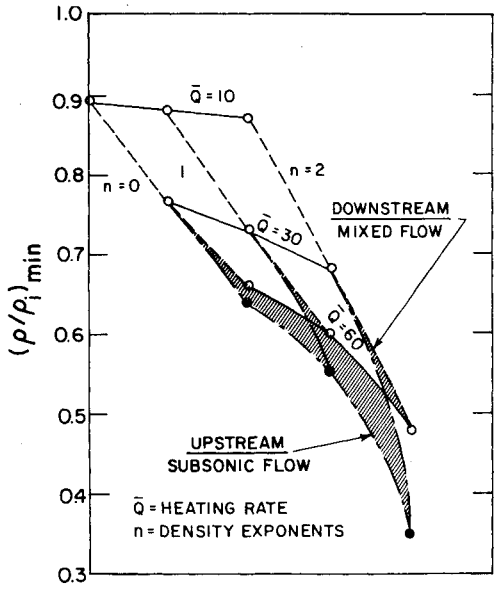

Fig. 10 One-dimensional minimum density map.

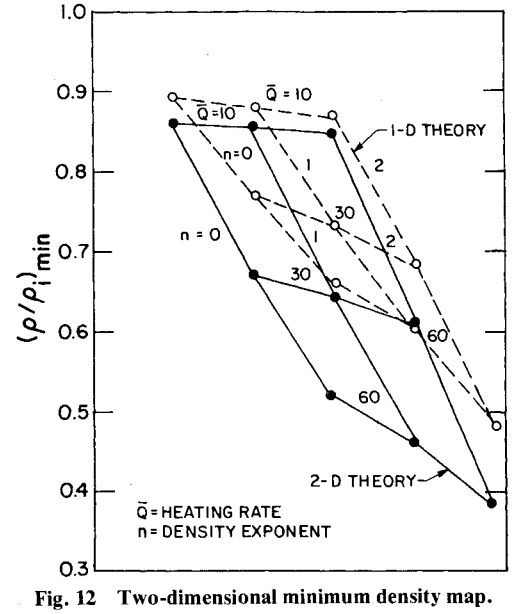

Fig. 12 Two-dimensional minimum density map.

because it is this point that will yield the maximum possible density decay rate and therefore is most vulnerable for initiation of an instability. It is observed that the minimum density in a two-dimensional sense occurs at the corner of the cathode/anode and e-beam shield while in a one-dimensional sense it occurs at the surface of the e-beam shield (assumed here to be a well-defined surface with perfect discharge confinement ability). Figure 9 shows the variation of minimum density with time for the one-dimensional case. Several values of the heating parameter ($\bar{Q}=10$, 30, and 60) were considered. We also considered different values of the exponent $n=1,2$. The results are plotted for upstream as well as downstream minimum density point. It is observed from the results shown in this figure that at low heating rates such as $\bar{Q}=10$, the coupling between plasma and fluid dynamics is not strong and therefore the density decay rate is slow. However, with increased heating rate $\bar{Q}$ and density exponent n, the density decay rate increases rapidly until a point in time when some other physical process tends to slow down the density decay rate. This phenomena was not found to be present in cases when the flow velocity remained subsonic everywhere until the end of a pulse time. This is observed in Fig. 9 and also in Fig. 10. In Fig. 10, we have replotted the results of Fig. 9 to show a map of normalized minimum density at the end of a pulse time for the one-dimensional case. It is more clearly evident from this figure that the density decay is more rapid when the local flow is subsonic. The explanation of this lies in the fact that the one-dimensional expansion process leads to a locally sonic situation for some conditions (such as $\bar{Q}=60$, $n=1$, 2 at the downstream location; see Fig. 9). Under these conditions, then, the acoustic waves can not propagate beyond this point, resulting in a decrease in density decay rate. This may well be an important mechanism for controlling the monotonic density decay rate in discharge in one-dimensional sense. Such a situation will not arise when one considers the two-dimensional effects. The minimum density as a function of time for this two-dimensional case is shown in Fig. 11. Notice that for the same heating rate the two-dimensional density decay rate is faster than that predicted by the one-dimensional case. However, the decay rate is not enhanced to a very dramatic level as one would expect. This behavior appears to be caused by the wave spreading effect in two dimensions. In principle one would be able to predict thermal instability in these discharges by noting very rapid changes in $d\rho/dt$ and ultimately $d\rho/dt$ approaching infinity (much the same way as in fluid-mechanical calculations involving flow separation, where the skin friction coefficient aproaches zero as the flow

approaches the separation point at a normal angle[29]). Such a situation will be observed as the density exponent n or the heating rate coefficient $\bar{Q}$ is increased (see Fig. 11). In Fig. 12 we have shown the two-dimensional effect discussed above as a map of minimum density for different parameters. The results obtained at the end of a pulse time for both the one-dimensional and the two-dimensional cases are shown in this figure. This gives an indication of the effect of longitudinal and transverse waves on the density exponentiation process. Note that the two-dimensional effects result in a greater stress enhancement as compared to the one-dimensional case. However the wave spreading effect tends to slow down the density decay rate in two dimensions.

V. Conclusions

This paper deals with discharge and flow characteristics of a typical electron-beam-controlled pulsed laser. Several aspects of the discharge problem, such as ionization source uniformity, discharge field uniformity, energy deposition uniformity, and discharge confinement, have been analyzed for one such device in order to demonstrate the usefulness of the theoretical predictions toward the laser cavity design. A self-consistent coupled numerical solution of the primary electron-beam scattering (and energy loss) problem and the sustainer discharge problem has been obtained to effectively address the issues. A numerical solution of this type has not been reported in the literature to date. From a flow standpoint an important aspect of laser discharges, which deals with the coupling between the cavity plasma and fluid dynamics, has been addressed to demonstrate the possibility of a thermal instability in such laser discharges. This has been achieved by developing a fluid mechanical model that accounts for plasma effects through a heat transfer term in the conservation equations. Numerical solution of these equations were obtained by using a shock capturing SHASTA algorithm. Parametric studies have been reported to demonstrate that this instability depends on the heat input into the cavity and the gas density exponent which provides the coupling between the plasma and fluid dynamics of the laser cavity. Possible physical processes that tend to restrict the growth of such instabilities are identified from the discussion of the theoretical results.

Acknowledgments

This research was supported jointly by the Army MIRADCOM and the Air Force Weapons Laboratory (AFWL) under Contract DAAK40-75-C-1272. Numerous technical discussions with Dr. J. H. Jacob are gratefully acknowledged.

References

[1] Reilly, J. P., "Pulser/Sustainer Electric-Discharge Laser," *Journal of Applied Physics*, Vol. 43, Aug. 1972, p. 3411.

[2] Daugherty, J. D., Pugh, E. R., and Douglas-Hamilton, D. H., *Bulletin of the American Physical Society*, Vol. 16, 1971, p. 399.

[3] Fernstermacher, C. A., Nutter, M. J., Rink, J. P., and Boyer, K., "Electron-Beam-Controlled Electrical Discharge as a Method of Pumping Large Volumes of CO_2 Laser Media at High Pressure," *Applied Physics Letters*, Vol. 20, Jan. 1972, p. 56.

[4] Finnebur, E. J., Fisher, H. N., Mason, R. J., and Morse, R. L., "Performance of DT Targets Exposed to Non-Optimized Laser Pulses," *Bulletin of the American Physical Society*, Vol. 18, 1973, p. 684.

[5] Jacob, J. H., Reilly, J. P., and Pugh, E. R., "Electron-Beam Spreading and Its Effect on Sustainer Current and Field Distribution in CO_2 Lasers," *Journal of Applied Physics*, Vol. 45, June 1974, p. 2609.

[6] Smith, R. C., "Computed Secondary-Electron and Electric Field Distributions in an Electron-Beam-Controlled Gas-Discharge Laser," *Applied Physics Letters*, Vol. 21, Oct. 1972, p. 352.

[7] Smith, R. C., "Use of Electron Backscattering for Smoothing the Discharge in Electron-Beam-Controlled Lasers; Computations," *Applied Physics Letters*, Vol. 25, Sept. 1974, p. 292.

[8] Boyer, K., Henderson, D. B., and Morse, R. L., "Spatial Distribution of Ionization in Electron-Beam-Controlled Discharge Lasers," *Journal of Applied Physics*, Vol. 44, Dec. 1973, p. 5510.

[9] Theophanis, G., Jacob, J. H., and Sackett, S., "Discharge Spatial Nonuniformity in E-Beam-Sustainer CO_2 Lasers," *Journal of Applied Physics*, Vol. 46, May 1975, pp. 2329-2331.

[10] Dutov, A. I., Mianev, S. V., and Nikolaev, V. B., "Optimization of the Electron Beam Parameters and Choice of the Foil in Electron-Beam-Controlled Lasers," *Soviet Journal of Quantum Electronics*, Vol. 9, Aug. 1979, pp. 995-1000.

[11] Cason, C., Perkins, J. F., Werkheiser, A. H., and Duderstadt, J., "E-Beam Spreading and Resulting Field Variations in CO_2 Laser Plasmas," *AIAA Journal*, Vol. 15, Aug. 1977, pp. 1079-1083.

[12] Bethe, H. A. and Jacob, J. H., "Diffusion of Fast Electrons in the Presence of an Electric Field," *Physical Review A*, Vol. 16, Nov. 1977, pp. 1952-1963.

[13] Jacob, J. H., Legner, H. H., Ahouse, D. R., and Wallace, J., "Medium Homogeneity Considerations in Low-Mach-Number Flow Discharges," *Applied Physics Letters*, Vol. 25, Nov. 1974, pp. 542-544.

[14] Jacob, J. H. and Mani, S. A., "Thermal Instability in High Power Discharges," *Applied Physics Letters*, Vol. 26, Jan. 1975, pp. 53-55.

[15] Douglas Hamilton, D. H. and Lowder, R. S., *AERL Kinetics Handbook*, AFWL TR-74-216, Air Force Weapons Laboratory, Kirtland Air Force Base, N. Mex., July 1974.

[16] Jacob, J. H., "Multiple Electron Scattering Through a Slab," *Physical Review A*, Vol. 8, July 1973, pp. 226-235.

[17] Jacob, J. H., "Penetration and Energy Deposition of Electrons in Thick Targets," *Journal of Applied Physics*, Vol. 45, Jan. 1974, pp. 467-475.

[18] Bethe, H. A., Rose, M. E., and Smith, L. P., *Proceedings of the American Philosophical Society*, Vol. 78, 1938, p. 753.

[19] Jacob, J. H., "Diffusion of Fast Electrons in the Presence of a Magnetic Field," *Applied Physics Letters*, Vol. 31, Aug. 1977, pp. 252-254.

[20] Henderson, D. B., "Electron Transport in Gas Discharge Lasers," Los Alamos Scientific Laboratory, Los Alamos, N. Mex., LA-5154-MS, April 1973.

[21] Henderson, D. B., "Electron Transport in Gas Discharge Lasers," *Journal of Applied Physics*, Vol. 44, Dec. 1973, pp. 5513-5516.

[22] Parazolli, C. G., "Electron-Beam-Stabilized Discharge in a Flowing Medium; Numerical Calculations," *AIAA Journal*, Vol. 16, 1978, pp. 592-599.

[23] Zienkiewicz, O. C., *The Finite Element Method*, McGraw-Hill Book Co., London, 1977.

[24] Sackett, S. J., Lawrence Livermore Laboratory, Livermore, Calif., Rept. 1778, 1978.

[25] "Electric Discharge Laser," Part II, Air Force Weapons Laboratory, N. Mex., Final Rept. AFWL-TR-75-162, Dec. 1975.

[26] Cobine, J. D., *Gaseous Conductors*, Dover Publications, N.Y., p. 136.

[27] Pugh, E. R., Wallace, J., Jacob, J. H., Northam, D., and Daugherty, J. D., "Optical Quality of Pulsed E-Beam Sustainer Laser," *Applied Optics*, Vol. 13, 1974, p. 2512.

[28] Book, D. L., Boris, J. P., and Main, K., "Flux-Corrected Transport II, Generalizations of the Method," *Journal of Computational Physics*, Vol. 18, 1975, pp. 248-283.

[29] Schlichting, H., *Boundary Layer Theory*, McGraw-Hill Book Co., New York, 1968.